Supporting Information

Enrichment and Recovery of Mammalian Cells From Contaminated Cultures Using Aqueous Two-phase Systems

Christopher J. Luby, Benjamin P. Coughlin, and Charles R. Mace*

Department of Chemistry, Tufts University, 62 Talbot Avenue, Medford, MA 02155 United States

*Corresponding author: charles.mace@tufts.edu

Contents:

Adhesion of *E. coli* to HeLa Cells

The recovered cell populations contained HeLa cells that had *E. coli* adhered to their surfaces **(Figure S2)**. We hypothesize that this adhesion was responsible for most of the *E. coli* that were still present in the recovered cell population because free *E. coli* would have sedimented to the container-ATPS interface based on density alone. Suspensions of HeLa cells that had recently been spiked with bacteria showed little to no bacterial adhesion, but cells incubated with bacteria for > 15 min showed the formation of bacteria-cell aggregates. We used cultures that had been incubated for > 30 min because these bacteria-cell aggregates more accurately reflect real-world contamination. To enhance separation efficiency, we attempted to remove the *E. coli* from the HeLa cells prior to adding them to the ATPS by washing them in various solutions. These solutions included surfactants (e.g., Pluronic F68, Jeffamine, Tween-20), blocking agents (skim milk), sugars (mannose and sialic acid) and ethylenediaminetetraacetic acid (EDTA). We also tried to remove the bacteria through physical (e.g., sonication, increased centrifugation speed) and enzymatic means (trypsin). We also adjusted the step in density in the ATPS to a lower density in order to pass cell aggregates through the system based on their increase in density in comparison to free HeLa cells. We also passed the suspension through the system more than once. None of these methods eliminated adhered bacteria from the recovered cell population (data not shown). We observed the same phenomenon with other adherent cell lines (3T3-L1, INS-1, MCF-7, and MDA-MB-231) and suspension cell lines (HL-60 II and Jurkat D1.1).

Image Processing

Images were imported from our microscopy software (Andor iQ3) as .tiff files and as .png files showing the overlay of GFP and RFP filters. This image was opened in Adobe Photoshop and the brightness and contrast were enhanced using the “Auto” feature. Images were compiled, sized, and marked up using Adobe Illustrator.

Table S1. Focused study on the reproducibility of density, osmolality, and pH of ATPS prepared from 7% (w/w) PEG and 11% (w/w) Ficoll. These values can be compared to the values obtained from generating the ATPS from a different stock solution each time (**Table 1**).

Top Phase				Bottom Phase			
Replicate	**Density** (g/mL)	**Osmolality** (mOsm/kg)	**pH**	**Replicate**	**Density** (g/mL)	**Osmolality** (mOsm/kg)	**pH**
1	1.0431	296	7.37	1	1.0762	296	7.42
2	1.0430	301	7.38	2	1.0762	305	7.37
3	1.0431	301	7.37	3	1.0762	304	7.42
4	1.0431	296	7.38	4	1.0762	302	7.43
5	1.0432	297	7.40	5	1.0762	304	7.39
6	1.0432	305	7.40	6	1.0761	305	7.39
7	1.0431	299	7.40	7	1.0762	300	7.39
8	1.0431	300	7.39	8	1.0762	297	7.41
9	1.0430	297	7.41	9	1.0763	298	7.41
10	1.0431	298	7.41	10	1.0761	305	7.37
Average	1.0431	299	7.39	**Average**	1.0762	302	7.40
Stdev	0.0001	3	0.02	**Stdev**	0.0001	4	0.02
SEM	0.0000	1	0.00	**SEM**	0.0000	1	0.01
%CV	0.01	0.9	0.21	**%CV**	0.01	1.2	0.29

Figure S1. Densities of cells and microorganisms determined by sink/float assays. Nycoprep was diluted to various concentrations to prepare a series of solutions with densities close to the reported densities of the cells and microorganisms used in this study. Cells were added to microcentrifuge tubes and centrifuged. The solutions were inspected for the presence of cells pelleted at the bottom, which would indicate that the density of the cell population was above that of the solution. HL-60 II and GFP-HeLa cells were stained with DiI to aid visualization of the cell pellet. Density ranges found using this sink/float method generally agree with values reported in the literature.

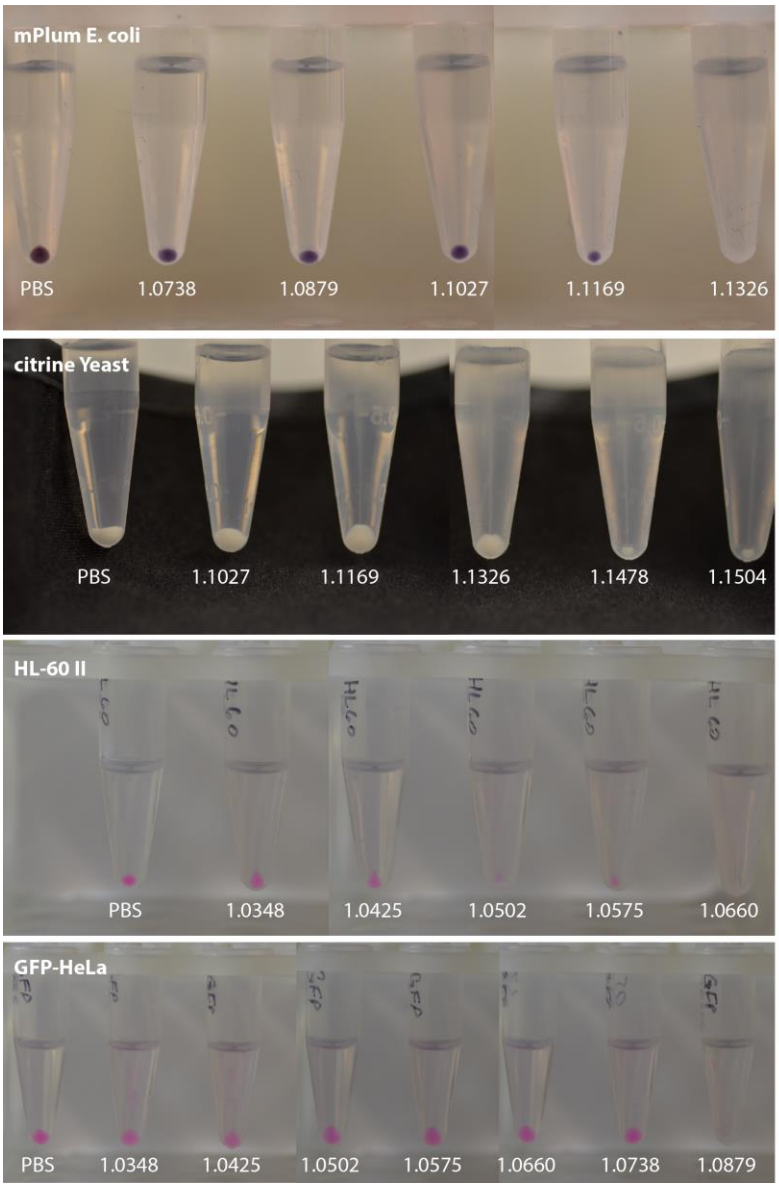

Figure S2. Time dependent adherence of *E. coli* to HeLa cells. When mPlum-expressing *E. coli* (red) are initially spiked into GFP-HeLa (green) cultures in suspension, there is little to no adhesion (**A**). After 15 minutes of incubation (**B**), most of the HeLa cells have many bacteria adhered to their surface. After passing cells through a PEG–Ficoll ATPS (**C** reproduced from Figure 3 in manuscript), there are still several cells with bacteria adhered to their surface in the recovered cell population (white arrows).

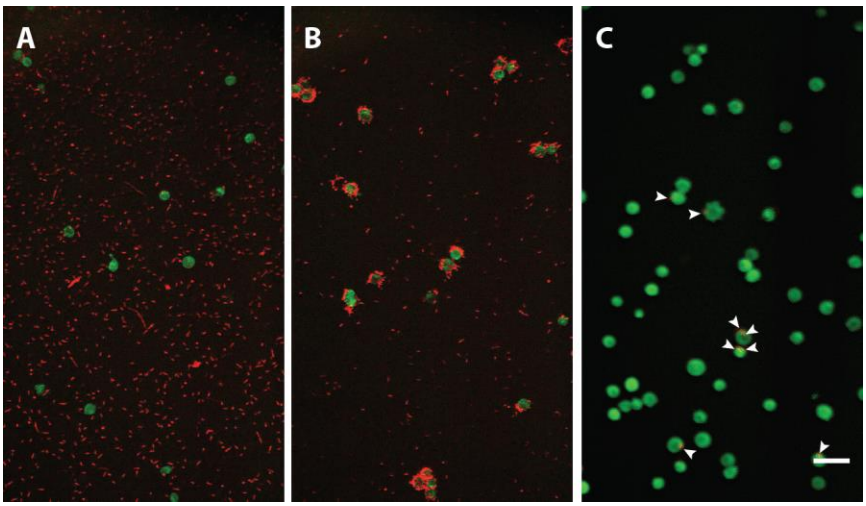

Figure S3. Flow cytometry data showing gating strategies for GFP-HeLa cells with mPlum *E. coli* adhered to their surfaces. Representative images shown for negative control (top), contaminated positive control (middle), and contaminated ATPS-treated sample (bottom).

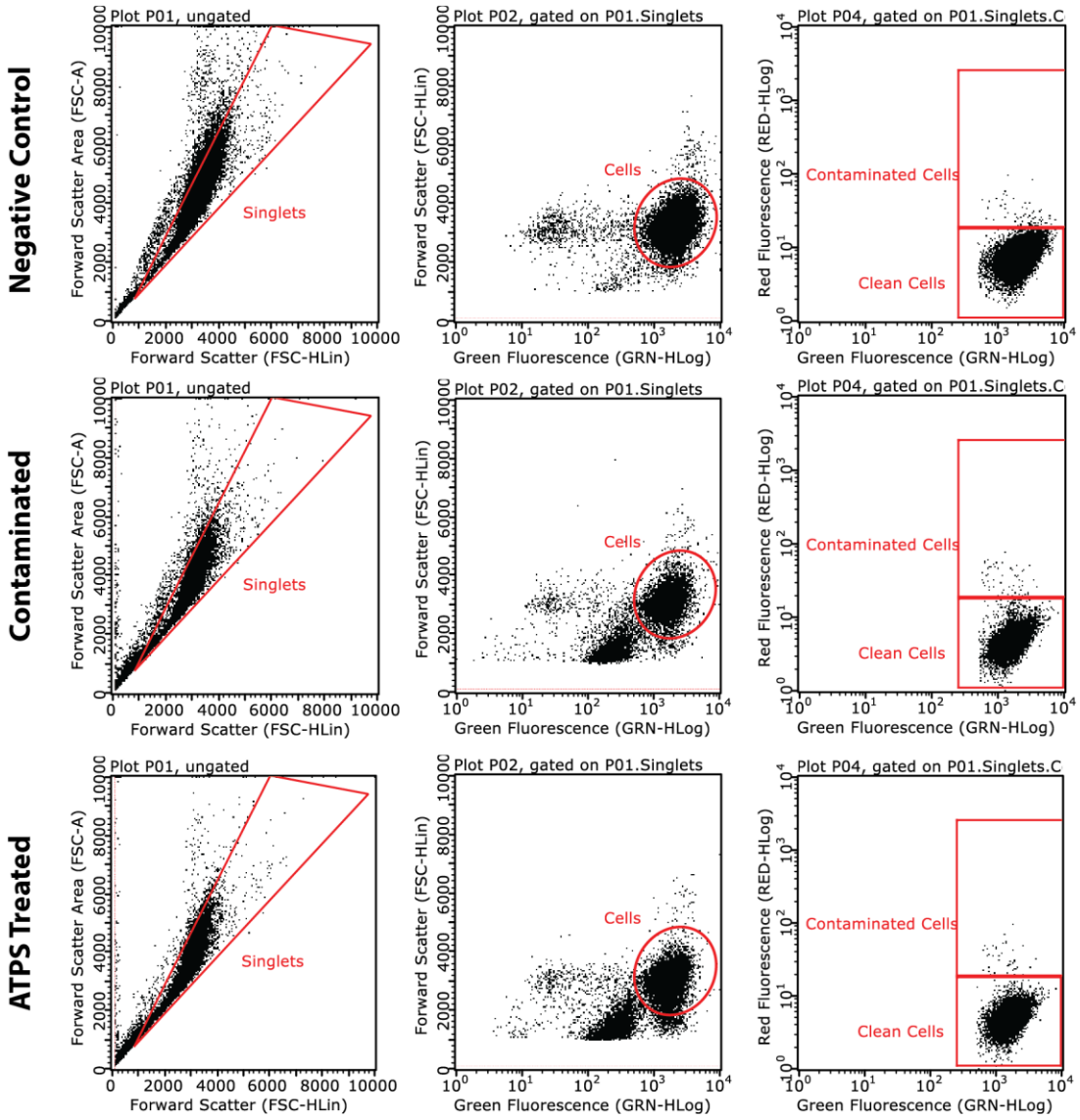

Figure S4. Flow cytometry data showing gating for total mPlum *E. coli*. Ungated scatter plots were divided into quadrants positive for green fluorescence and far red fluorescence. All events in the two top quadrants were considered bacteria. Representative images of negative control, positive (contaminated) control, and ATPS treated samples are shown from trial 1.

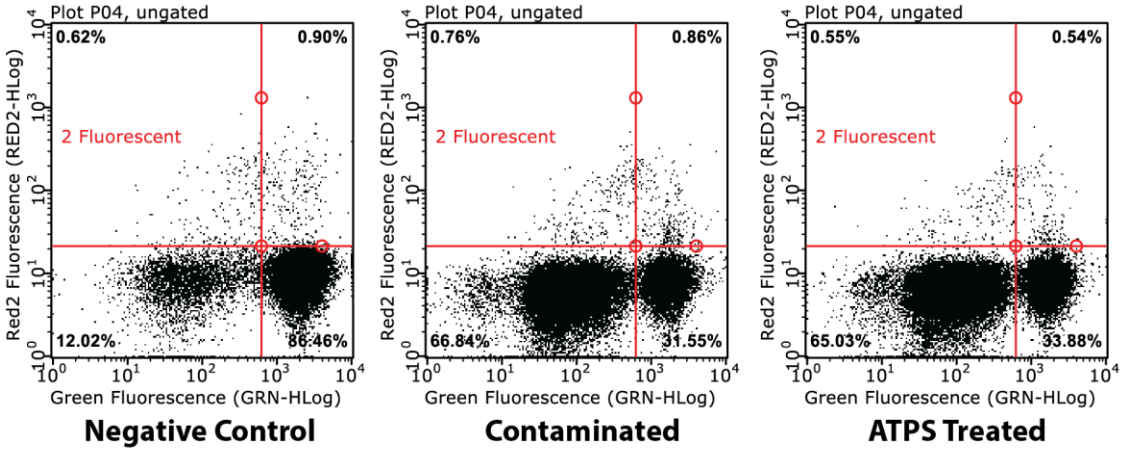

Figure S5. Colony formation assays. (A, B) Representative images from a colony formation assay to determine the total colony forming units (CFU)/mL present in contaminated culture of HeLa cells before and after treatment with a PEG–Ficoll ATPS. (C, D) Images from ImageJ showing automated identification of individual colonies.

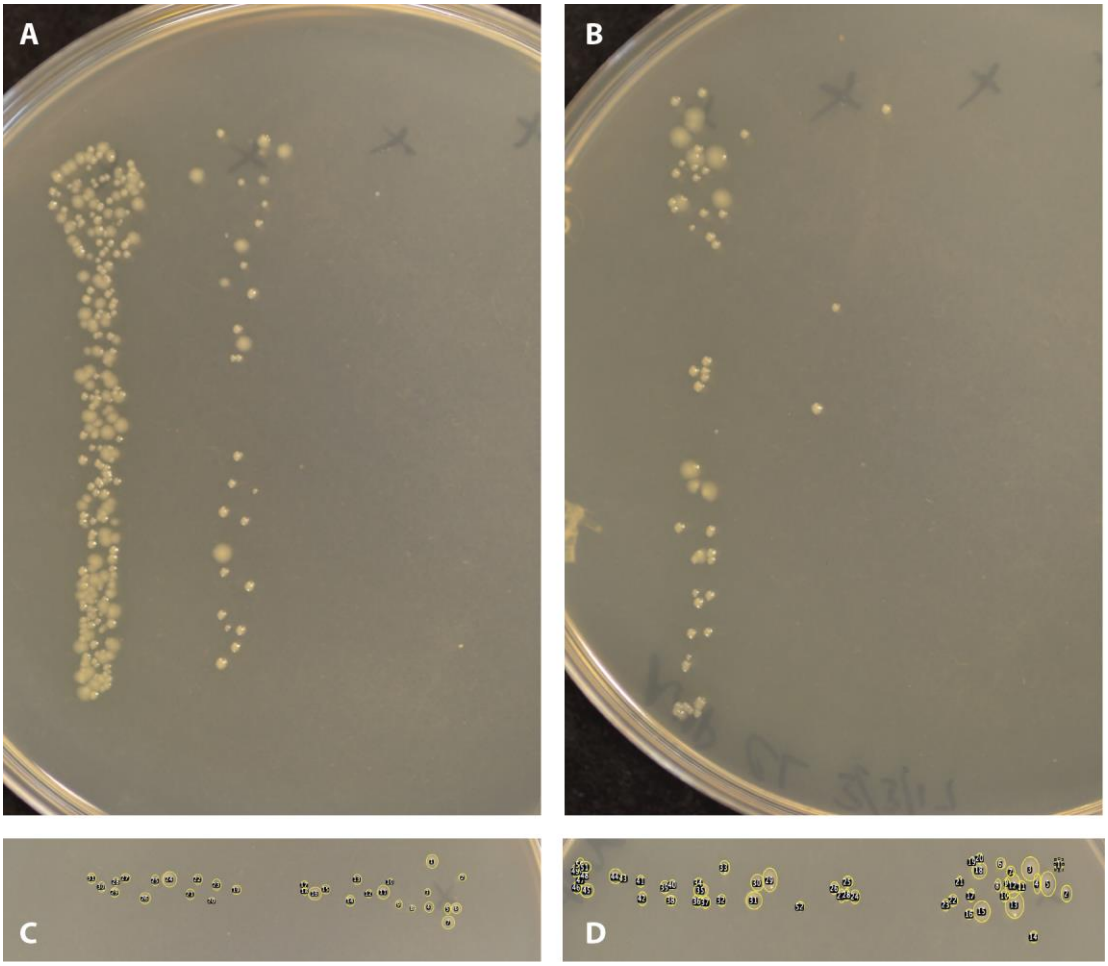

Figure S6. Percent recovery as a function of cells added to the ATPS. We observe a positive correlation (r = 0.81) between the number of cells added and the percent of cells recovered.

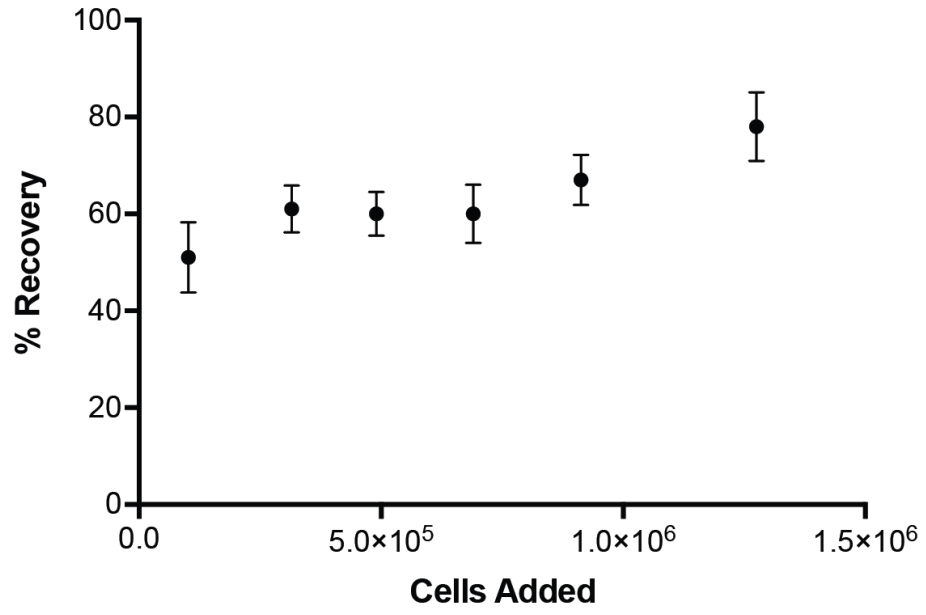

Figure S7. Separation of mPlum *E. coli* from DiO-stained HL-60 II cells. Cell populations are first gated for single cells and then divided into quadrants that are positive for each of the fluorophores present. Controls show the positions of unstained cells, stained cells, and contaminated cells. Treat cell populates are enriched for HL-60 II cells, removing 58% of the contaminants on average.

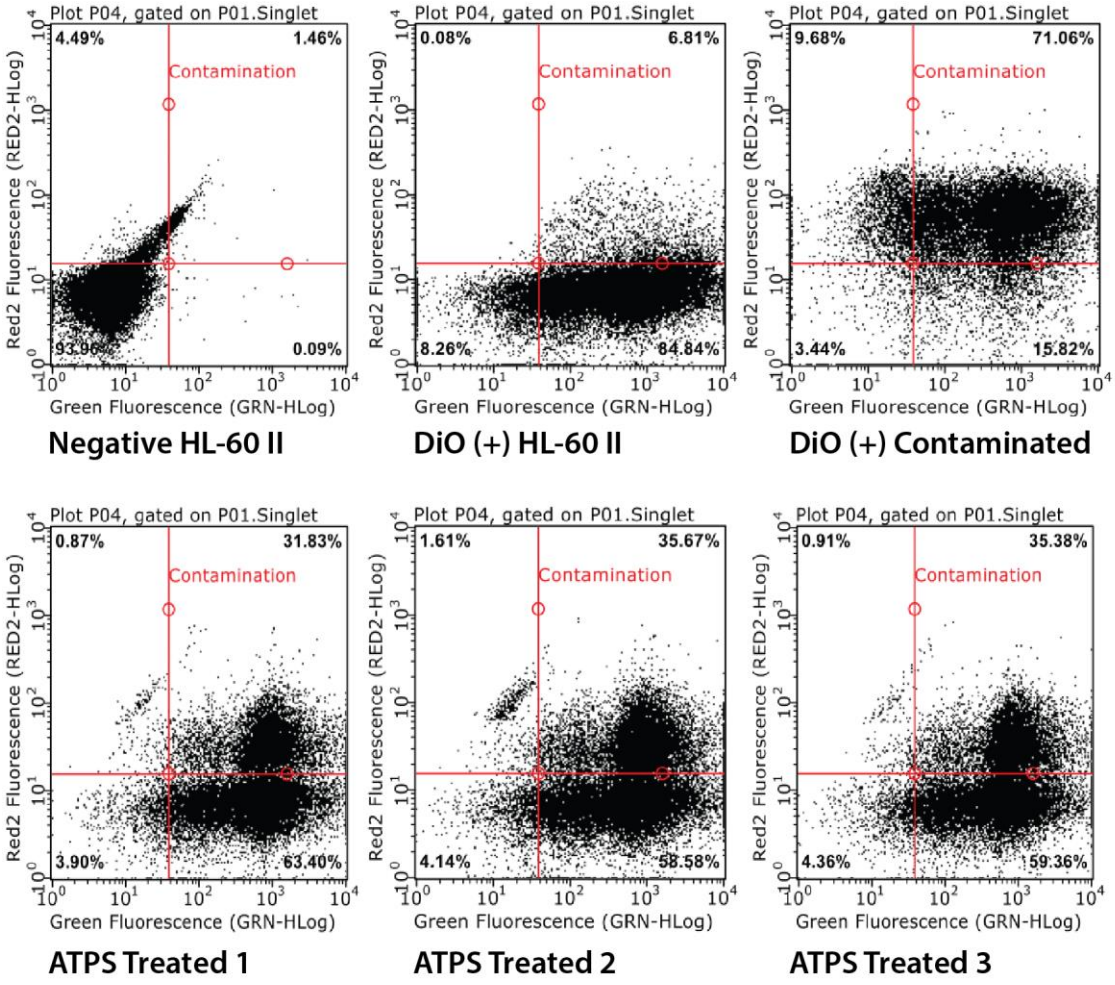

Figure S8. Separation of citrine-expressing yeast from DiI-stained HeLa cells. Cell populations are first gated for single cells and then divided into quadrants that are positive for each of the fluorophores present. Controls show the positions of unstained cells, stained cells, and contaminated cells. Treat cell populates are enriched for HeLa cells, removing 32% of the contaminants on average.

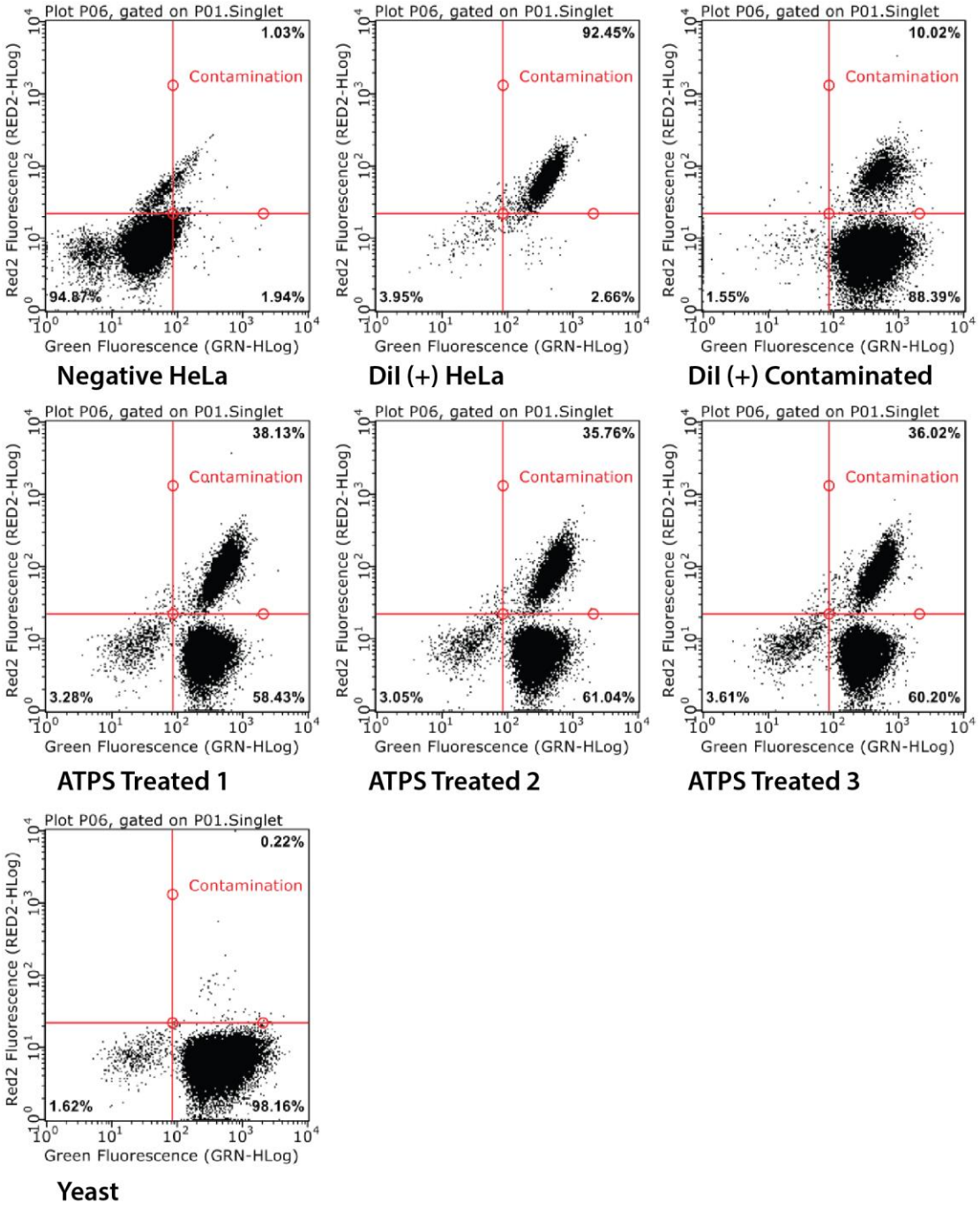

Figure S9. Separation of citrine-expressing yeast from DiI-stained HL-60 II cells. Cell populations are first gated for single cells and then divided into quadrants that are positive for each of the fluorophores present. Controls show the positions of unstained cells, stained cells, and contaminated cells. Treat cell populates are enriched for HL-60 II cells, removing 50% of the contaminants on average.

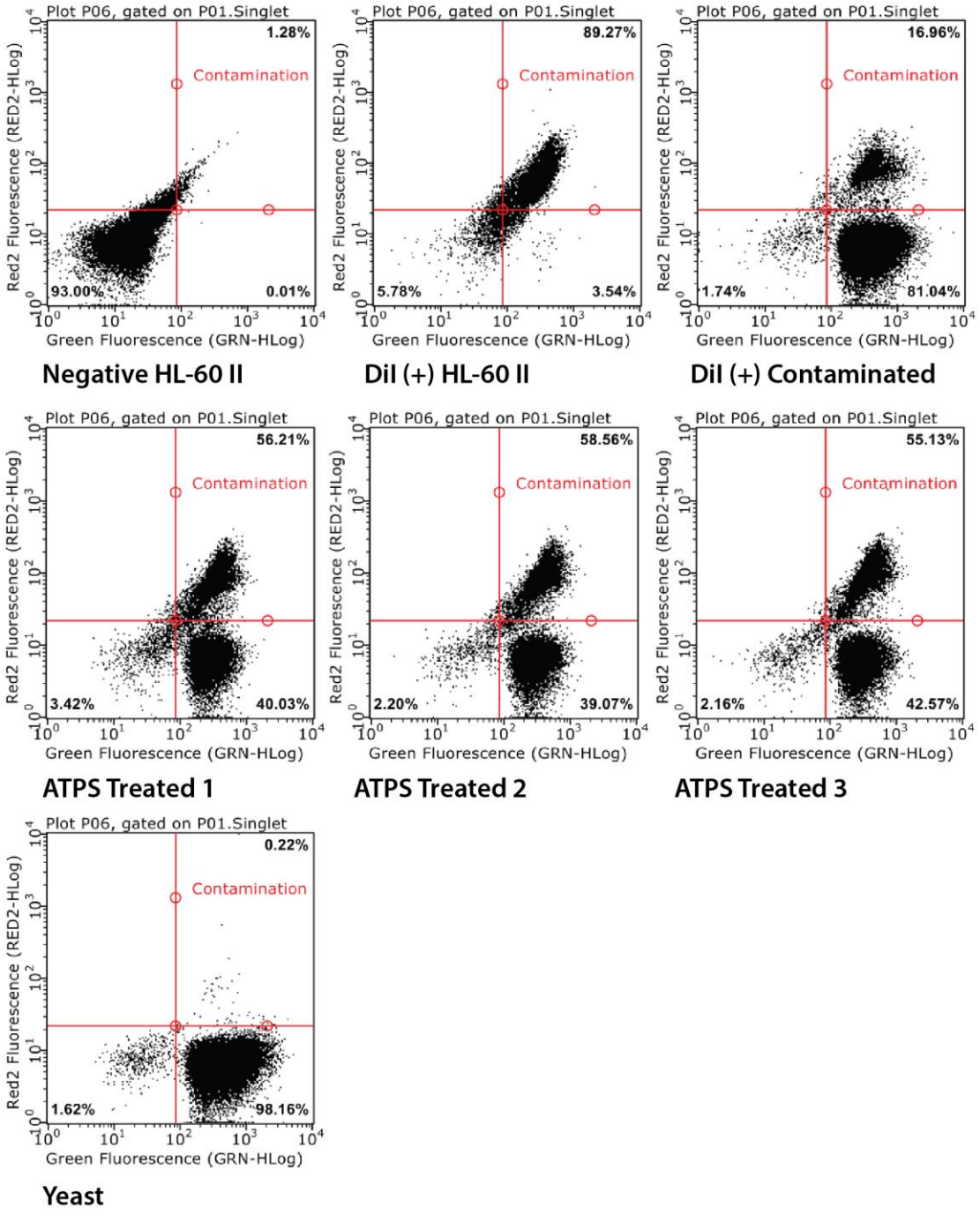

Figure S10. Image of a PEG-Ficoll ATPS after centrifugation with DiI-stained HL-60 II cells. The recoverable cells are clearly visible as a band at the liquid-liquid interface due to their bright red color. There is also some colored species observable at the medium-ATPS boundary and the bottom of the container. This would account for some of the cells that are not recovered during the assay. It is also clear from this image that the ATPS is largely undisturbed by the addition of a layer of cells and culture medium.